



Published in final edited form as:

*J Neuroendocrinol.* 2020 November ; 32(11): e12854. doi:10.1111/jne.12854.

## GHR<sup>-/-</sup> Mice are Protected from Obesity-Related White Adipose Tissue Inflammation

Jonathan A. Young<sup>a,b,\*</sup>, Brooke E. Henry<sup>a,c,d,\*</sup>, Fabian Benencia<sup>b</sup>, Stephen Bell<sup>d</sup>, Edward O. List<sup>a</sup>, John J. Kopchick<sup>a,b</sup>, Darlene E. Berryman<sup>a,b,d,†</sup>

<sup>a</sup>Edison Biotechnology Institute, Ohio University, Athens, OH 45701, USA.

<sup>b</sup>Department of Biomedical Sciences, Heritage College of Osteopathic Medicine, Ohio University, Athens, OH 45701, USA.

<sup>c</sup>School of Applied Health Sciences and Wellness, College of Health Sciences and Professions, Ohio University, Athens, OH 45701, USA.

<sup>d</sup>The Diabetes Institute at Ohio University, Ohio University, Athens, OH 45701, USA.

### Abstract

Growth hormone (GH) excess in bovine (b)GH transgenic mice has been shown to alter white adipose tissue (WAT) immune cell populations. The current study aimed to evaluate the effects of GH resistance on WAT immune cell populations using GH receptor knockout (GHR<sup>-/-</sup>) mice. Eight- and 24-month-old, male GHR<sup>-/-</sup> and wild type mice were used. Body composition and tissue weights were determined, and systemic inflammation was assessed by measuring serum cytokine levels. The stromal vascular fraction (SVF) was isolated from three distinct WAT depots, and immune cell populations were quantified using flow cytometry. GHR<sup>-/-</sup> mice at both ages had decreased body weight but were obese. While no significant changes were observed in serum levels of the measured cytokines, SVF cell alterations were seen and differed from depot to depot. Total SVF cells were decreased in epididymal (Epi), while SVF cells per gram adipose tissue weight were increased in mesenteric (Mes) of GHR<sup>-/-</sup> mice relative to controls. T cells and T helper cells were increased in Mes at 8 months old, while cytotoxic T cells were decreased in subcutaneous (SubQ) at 24 months old. Other cells were unchanged at both ages measured. This study demonstrates that removal of GH action results in modest and depot-specific changes to several immune cell populations in WAT of intra-abdominal depots (Epi and Mes), results that are somewhat surprising because the SubQ has the largest change in size, while the Mes has no size change. Taken together with previous results from bGH transgenic mice, these data suggest that GH induces changes in the immune cell population of WAT in a depot-specific manner. Notably, GHR<sup>-/-</sup> mice appear to be protected from age-related WAT inflammation and immune cell infiltration despite obesity.

† Corresponding Author at: Edison Biotechnology Institute, Ohio University, Athens, OH 45701, USA. berrymad@ohio.edu.

\*These authors contributed equally to this work

## Keywords

White adipose tissue; WAT; GHR<sup>-/-</sup> mice; stromal vascular fraction; SVF; leukocyte; T-cells; adipose tissue macrophages; ATM

---

## 1. Introduction

An interaction between the somatotrophic axis and immune system is well documented. This interaction was first described in rats in the 1930s in which hypophysectomy was reported to accelerate the rate of thymic involution (1). More recently, data from several mouse lines with altered GH action show further alterations in immune function. For example, in the Snell and Ames dwarf mice, which show multiple pituitary deficiencies including GH, the humoral and cell mediated immune response is impaired but can be reversed with GH treatment (2). Likewise, mice with an excess in GH, such as bovine GH transgenic (bGH) mice, have increased T cell differentiation and migration in blood, thymus and spleen (3–5). Clinical conditions of altered GH action, such as GH deficiency and acromegaly, also result in altered inflammatory status, which is indicative of changes in immune function (6). Although there is a clear link between the somatotrophic axis and immune function, the importance of these changes and their influence on immune cells within white adipose tissue (WAT) have yet to be fully evaluated.

White adipose tissue (WAT) serves as an important energy reservoir and has been shown to possess an adaptable immune cell population that contributes to the metabolic and endocrine functions of the tissue (7). The immunological properties of WAT are clearly illustrated in the changes that occur with obesity. In an obese state, WAT expansion is accompanied by infiltration of immune cells (such as cytotoxic T cells and macrophages) and phenotypic switching of resident immune cells (such as anti-inflammatory M2 macrophages to inflammatory M1)(8–10). Collectively, these observations suggest a dynamic situation in which immune cells are recruited to WAT and participate in remodeling and inflammation of the tissue. With advanced age, WAT mass tends to shift from subcutaneous (SubQ) to visceral depots (11). Along with this shift in location comes a shift in the immune cell profile in the tissue. Aged mice have a decrease in M2 macrophages, and coinciding with the changes in macrophage population is an increase in T cell population in the epididymal WAT, including the T helper and cytotoxic T cell subsets (11). As a whole, aged mice tend to have increased WAT inflammation.

In addition to a role in immune function, GH is well known to alter WAT, promoting lipolysis and inhibiting lipogenesis in a depot specific manner. For example, several mouse lines with a decrease or absence in GH action, such as GHR<sup>-/-</sup> mice, have a distinct accumulation of WAT in the SubQ depot along with an increase in adipocyte size (11–13). However, few published studies have investigated the role of GH on WAT immune cell populations. One example includes the MacGHRKO mouse line, in which the GHR gene is disrupted in macrophages; in these mice, AT macrophages are polarized to the inflammatory M1 phenotype in the epididymal depot (14). Even fewer studies examine multiple adipose depots. One study reports that GHR<sup>-/-</sup> have reduced IL-6 levels in perinephric and

epididymal (Epi) AT relative to normal mice (15). At the other extreme, excess GH action in bGH mice reveal greater macrophage and regulatory T-cell infiltration in SubQ and mesenteric (Mes) WAT depots when compared with controls (16). Additionally, this study provides results from RNA sequencing that confirmed T-cell infiltration and activation pathways are increased in the SubQ depot of bGH mice. Collectively, these studies show alterations in WAT immune cell number or phenotype due to GH although not all have explored depot differences and most focused solely on the macrophage populations (17–19).

Growth hormone receptor knockout mice (GHR<sup>-/-</sup>) represent a unique model of “healthy obesity.” That is, they have increased adiposity due to a preferential increase in SubQ WAT, enhanced insulin sensitivity, and are long lived (20–24). While there is published evidence that macrophages are decreased in the SubQ depot of GHR<sup>-/-</sup> mice (17), a survey of the subsets of macrophages and other immune cells in various depots of GHR<sup>-/-</sup> mice is needed to better understand how these cells may contribute to the health of this tissue and the animal. Therefore, to complement a previous study with bGH mice (16) and to better understand the immune cell populations, we sought to determine if a lack of GH action alters WAT immune cell populations in different depots and at different ages. To do this, SVF cells, total leukocytes, T cell subsets (T helper and cytotoxic) and ATMs (M1 and M2) were quantified in SubQ, Epi, and Mes WAT of GHR<sup>-/-</sup> and littermate control mice at 8 and 24 months of age.

## 2. Materials and methods

### 2.1 Animals

GHR<sup>-/-</sup> mice in the C57BL/6J background strain were bred at Edison Biotechnology Institute of Ohio University as previously described (24). Eight male GHR<sup>-/-</sup> mice and eight male wild type littermate controls at 8 and 24 months of age were used. Mice were housed 2–4 per cage in controlled 14-hour light/10-hour dark cycles at 22 ± 2 °C, and standard rodent chow (ProLab RMH 3000, PMI Nutrition International, Inc., St. Louis, MO) and water were provided *ad libitum*. All animal procedures were approved by the Ohio University Institutional Animal Care and Use Committee.

### 2.2 Body weight and body composition

Body weight and body composition were measured 1 day prior to dissection. Body composition measurements for fat, free body fluid, and lean tissue were collected using a quantitative nuclear magnetic resonance (NMR) apparatus (Bruker Minispec) according to methods previously described (25–27).

### 2.3 Stromal vascular fraction isolation

Three fat depots were examined in this study. These include inguinal subcutaneous (SubQ), Epididymal (Epi) and Mesenteric (Mes). Mice were bled retroorbitally and killed by cervical dislocation prior to dissection. Blood was kept on ice until processing. Immediately after dissection, WAT depots were weighed and placed on ice in a conical tube containing Krebs-Henseleit buffer. SVF isolation was performed according to previously established methods with slight modifications (16). Briefly, WAT samples were minced and treated with 2.5

mg/ml of type II collagenase (Sigma-Aldrich, St. Louis, MO). Samples were then placed in a shaking incubator at 37 °C for approximately 20 min at 200–300 rpm. Samples were filtered through 100 µm mesh strainers (Fisherbrand) and centrifuged at 500xg for 10 min at 4 °C to separate the adipocytes from the SVF portion. Final pellets were suspended in 180 µl of FACS blocking buffer [FACS buffer: 1X phosphate buffered saline, 2% characterized fetal bovine serum (HyClone™) and 0.05% sodium azide plus 10% horse serum (Life Technologies™) plus CD16/32 (93) from eBioscience, San Diego, CA at a 1:100 dilution] to prevent nonspecific binding.

## 2.4 Flow cytometry

Samples were stained with monoclonal anti-mouse antibodies according to a previously developed staining protocol (16). Fluorochrome-conjugated monoclonal antibodies (Tables 1 and 2) were used in this study followed by incubation with streptavidin eFluor® 615 at a 1:200 dilution. All antibodies were used at the manufacturer recommended dilution. Isotype and fluorescence minus one (FMO) controls were also used. Samples were stored in Cytotfix™ (BD Biosciences) and subjected to multicolor flow cytometry the following day on the FACS Aria (8 months) or MACSQuant 10 (24 months) flow cytometer. Approximately 10,000–100,000 events were collected per sample. Results were analyzed with FlowJo V10 software.

## 2.5 Serum Cytokines

Blood collected at dissection was allowed to clot at room temperature for 30 minutes, followed by centrifugation at 8000xg for 10 minutes at 4°C. The serum was transferred to a new tube for storage at –80°C; serum measurements were performed from samples collected at 8 and 24 months of age. IL-6, monocyte chemoattractant protein 1, and TNF-α were measured using a mouse metabolic magnetic bead panel (catalog no. MMHMAG-44K; MilliporeSigma, Burlington, MA). Other cytokines were measured using a mouse cytokine/chemokine metabolic bead panel (catalog no. MCYTOMAG-70K-PMX). Kits were completed according to the manufacturers' instructions.

## 2.6 Statistical Analysis

GraphPad Prism 7.0 was used for statistical analysis. All group means were reported as mean ± SEM. Independent t tests were used to evaluate each data set and determine if there were any differences between WT and GHR<sup>-/-</sup> mice. For data that violated the assumptions of equal variances, a Welch's t test was performed. When data violated the assumption of normality, the Mann-Whitney U test was performed. For comparisons between different ages of mice, a one-way ANOVA with Tukey's post-hoc test was used. For all tests, p<0.05 was considered significant.

## 3. Results

### 3.1 Body weight, body composition, tissue weight and serum cytokine levels

To characterize the immune cell population in adult mice and to be able to compare results with our previous study in bGH mice, we initially started with 8 month old GHR<sup>-/-</sup> mice. Body weight of GHR<sup>-/-</sup> mice was significantly decreased (61% decrease) at 8 months of

age as compared to littermate controls (Figure 1A;  $p < 0.0001$ ,  $t = 22.17$ ,  $df = 13$ ). Because of the large difference in body weight between the genotypes, body composition data are normalized to body weight. Fat mass was doubled GHR<sup>-/-</sup> mice (Figure 1B;  $p < 0.0001$ ,  $t = 10.47$ ,  $df = 13$ ), while lean mass (Figure 1B) was significantly decreased (an 11% decrease;  $p = 0.0004$ ,  $t = 4.773$ ,  $df = 13$ ), and normalized fluid mass was not significantly different from WT mice (Figure 1B;  $p = 0.1218$ ,  $t = 1.655$ ,  $df = 13$ ). When looking at individual depots, there was no difference in the absolute mass of SubQ (WT  $0.6 \pm 0.1$ , GHR<sup>-/-</sup>  $0.7 \pm 0.1$ ;  $p = 0.17$ ); however, Epi and Mes were significantly decreased in GHR<sup>-/-</sup> mice (Epi: WT  $1.1 \pm 0.2$ , GHR<sup>-/-</sup>  $0.2 \pm 0.02$ ;  $p = 6.6 \times 10^{-11}$  Mes: WT  $0.4 \pm 0.1$ , GHR<sup>-/-</sup>  $0.1 \pm 0.02$ ;  $p = 0.006$ ). When normalized as percent of body weight, SubQ was tripled in GHR<sup>-/-</sup> compared to WT ( $p < 0.0001$ ,  $t = 9.126$ ,  $df = 13$ ), while Epi was decreased by half ( $p = 0.0018$ , Welch-corrected  $t = 4.326$ ,  $df = 9.289$ ), and there was a significant 26% decrease in Mes (Figure 1C;  $p = 0.0401$ ,  $U = 10$ ).

To assess the systemic inflammation in 8-month old GHR<sup>-/-</sup> mice, serum levels of 3 cytokines (IL-6, MCP-1, and TNF $\alpha$ ) were assessed (Figure 1D). No significant changes in any of these cytokines were observed in the GHR<sup>-/-</sup> mice, but mean circulating TNF $\alpha$  in GHR<sup>-/-</sup> mice was 50% of that in controls (Fig 1D; TNF $\alpha$   $p = 0.075$ ,  $t = 1.937$ ,  $df = 13$ ; IL-6  $p = 0.3969$ ,  $U = 20$ ; MCP-1  $p = 0.2654$ ,  $t = 1.937$ ,  $df = 13$ ). Of note there was a significant increase in G-CSF and decrease in IL-1 $\alpha$  and KC in the serum of GHR<sup>-/-</sup> at this age. (Supplemental Figure 5)

### 3.2 Stromal vascular fraction quantification

There was no difference in the number of SVF cells isolated from SubQ and Mes in 8 month old GHR<sup>-/-</sup> as compared to WT (SubQ: WT  $1.4 \times 10^5 \pm 3 \times 10^4$ , GHR<sup>-/-</sup>  $1.6 \times 10^5 \pm 2.7 \times 10^4$ ;  $p = 0.6525$ ,  $t = 0.4601$ ,  $df = 14$ . Mes: WT  $4.2 \times 10^5 \pm 7.2 \times 10^4$ , GHR<sup>-/-</sup>  $2.3 \times 10^5 \pm 5.3 \times 10^4$ ;  $p = 0.0537$ ,  $t = 2.106$ ,  $df = 14$ ); however, the number of SVF cells from Epi was significantly decreased in GHR<sup>-/-</sup> relative to WT (WT:  $3.2 \times 10^5 \pm 6.9 \times 10^4$ , GHR<sup>-/-</sup>:  $9.9 \times 10^4 \pm 2.2 \times 10^4$ ,  $p = 0.0171$ , welch-corrected  $t = 3.078$ ,  $df = 7.249$ ). As in other studies of WAT immune cells in obese states, (28) due to the difference in the size of the WAT depots in GHR<sup>-/-</sup> mice, immune cell data were then normalized to tissue weight. In this analysis, the only significant genotype difference was in Mes, in which GHR<sup>-/-</sup> mice had significantly increased (121%;  $p = 0.014$ ,  $U = 7$ ) SVF cells/g of tissue (Figure 2A; SubQ  $p = 0.6903$ ,  $t = 0.4075$ ,  $df = 13$ ; Epi  $p = 0.2552$ ,  $t = 1.2$ ,  $df = 11$ ).

### 3.3 Quantification of immune cells

**3.3.1 -Leukocytes—**Leukocytes were identified as CD45<sup>+</sup> cells. CD45<sup>+</sup> MHCII<sup>+</sup> cells were considered antigen presenting cells (which includes overall macrophages, B cells and dendritic cells). There were no statistically significant differences in leukocytes and antigen presenting cells in GHR<sup>-/-</sup> mice relative to controls in any depot at 8 months of age (Figure 2 B–C; Leukocyte SubQ  $p = 0.6943$ ,  $U = 24$ ; Epi  $p = 0.1226$ , Welch-corrected  $t = 1.705$ ,  $df = 8.955$ ; Mes  $p = 0.2345$ ,  $U = 20$ ; Antigen-presenting cell SubQ  $p = 0.4634$ ,  $U = 21$ ; Epi  $p = 0.065$ ,  $U = 14$ ; Mes  $p = 0.6454$ ,  $U = 27$ )).

**3.3.2 -T cells**—Total T cells included all CD3<sup>+</sup>CD45<sup>+</sup> cells. In figure 3B, the number of T cells per gram of WAT is shown. This corresponds to the histograms in figure 3A, which shows the relative intensity of CD3<sup>+</sup> and CD45<sup>+</sup> used to quantify T cells. A significant increase (115%;  $p=0.0281$ ,  $U=11$ ) in Mes T cells was observed in GHR<sup>-/-</sup> compared to WT animals at 8 months of age (Figure 3 A–B: SubQ  $p=0.4634$ ,  $U=21$ ; Epi  $p=0.1304$ ,  $U=17$ ). There were no statistically significant genotype differences in the number of T cells in the other depots.

T helper cells, which are required for almost all immune responses as they promote adhesion to target and antigen presenting cells (APCs), were identified as CD45<sup>+</sup>CD3<sup>+</sup>CD4<sup>+</sup> (Figure 4A). A statistically significant increase in T helper cells was only observed in the GHR<sup>-/-</sup> Mes depot (Mes 118% increase;  $p=0.0148$ ,  $U=9$ ; SubQ  $p=0.9551$ ,  $U=27$ ; Epi  $p=0.4347$ ,  $t=0.8042$ ,  $df=14$ ) compared to controls. Cytotoxic T cells were identified as CD45<sup>+</sup>CD3<sup>+</sup>CD4<sup>-</sup> cells in the 8 month cohort (Figure 4B) and have the ability to directly kill infected cells and contribute to obesity-related inflammation that precedes macrophage infiltration to WAT (29). GHR<sup>-/-</sup> animals had twice the number of cytotoxic T cells in the Mes depot compared to controls at 8 months of age but this increase was not statistically significant (Mes  $p=0.0662$ ,  $t=1.993$ ,  $df=14$ ; SubQ  $p=0.9551$ ,  $U=27$ ; Epi  $p=0.2786$ ,  $U=21$ ). No other statistically significant changes in T helper cells or cytotoxic T cells were observed.

**3.3.3 -Adipose tissue macrophages**—Adipose tissue macrophages (ATMs) were identified as CD45<sup>+</sup>MHC-II<sup>+</sup>F4/80<sup>+</sup>. GHR<sup>-/-</sup> mice had no significant changes in ATMs/g of tissue compared to controls (Figure 4C: SubQ  $p=0.4634$ ,  $U=21$ ; Epi  $p=0.4418$ ,  $U=24$ ; Mes  $p=0.1679$ ,  $t=1.454$ ,  $df=14$ ). Because of the heterogeneity of macrophage phenotypes, ATMs were further classified as anti-inflammatory, M2 (CD45<sup>+</sup>F4/80<sup>+</sup>CD206<sup>+</sup>) or pro-inflammatory, M1 (CD45<sup>+</sup>F4/80<sup>+</sup>CCR2<sup>+</sup> in 8 month cohort and CD45<sup>+</sup>F4/80<sup>+</sup>CD38<sup>+</sup>CD80<sup>+</sup> in 24 month cohort). Both populations have been implicated in regulating the WAT microenvironment (30). No significant changes were observed between GHR<sup>-/-</sup> mice and controls in M1 (SubQ  $p=0.2319$ ,  $U=17$ ; Epi  $p=0.1944$ ,  $U=19$ ; Mes  $p=0.3823$ ,  $U=23$ ) or M2 (SubQ  $p=0.28$ ,  $t=1.127$ ,  $df=13$ ; Epi  $p=0.3823$ ,  $U=23$ ; Mes  $p=0.1605$ ,  $U=18$ ) macrophages at 8 months of age (Figure 5).

### 3.4 Aged (24 Month) Cohort

Because dramatic changes in immune cells were not apparent at 8 month of age and because GHR<sup>-/-</sup> mice have extended longevity, we next evaluated the immune cell population in aged adult mice at 24 months of age. Due to the differences in the antibodies used and gating strategy, direct comparisons between the 8 month and 24 month cohort cannot be made; however, these data provide an opportunity to examine general trends. At 24 months of age, body composition results showed similar trends to the 8 month results. That is, body weight was 68% decreased in GHR<sup>-/-</sup> mice (Figure 6A;  $p<0.0001$ ,  $t=12.95$ ,  $df=12$ ), and fat mass was significantly increased (196%;  $p<0.0001$ ,  $t=5.815$ ,  $df=12$ ) (Figure 6B). There were corresponding decreases in lean mass (18.67%,  $p=0.0006$ ,  $U=0$ ) and fluid mass (7.05%,  $p=0.0024$ ,  $t=3.826$ ,  $df=12$ ); however, there were no significant differences in depot weights at

24 months of age (Supplemental Figure 1), although GHR<sup>-/-</sup> mice had 219% increase in SubQ (p=0.1649, U=13).

At 24 months, there was no difference between GHR<sup>-/-</sup> and controls in the serum levels of IL-6, MCP-1 or TNF- $\alpha$  (Figure 6C: IL-6 p=0.6402, U=27; MCP-1 p=0.2092, Welch-corrected t=1.356, df=8.704; TNF- $\alpha$  p=0.4462, U=24.5), and there were no significant differences comparing 8 month mice to 24 month mice by one-way ANOVA. (IL-6 F<sub>30</sub>=3.388 p=0.0324 (no significant differences in pairwise tests), MCP-1 F<sub>31</sub>=1.577 p=0.218, TNF- $\alpha$  F<sub>31</sub>=1.251 p=0.3109) In the aged mice, there was once again a significant decrease in absolute SVF cells in GHR<sup>-/-</sup> Epi but no change when normalized to tissue weight. There were no changes in total T cells, T helper cells, or M1 or M2 macrophages (Supplemental Figures 2–4). The only significant difference between GHR<sup>-/-</sup> mice and controls was a 93% decrease (p=0.0105, U=5.5) in Cytotoxic T cells in the SubQ depot of GHR<sup>-/-</sup> mice (Figure 6D).

#### 4. Discussion

The goal of this study was to quantify select immune cell populations within WAT in adult GHR<sup>-/-</sup> male mice. Our data show that the immune cells of the Mes depot are the most profoundly affected by a lack of GH action, at least at 8 months of age, while those in the SubQ depot are relatively unaffected by the lack of GH signaling. The lack of change in the SubQ is surprising because it is the most changed in size (enlarged) in GHR<sup>-/-</sup> mice. In contrast, the tissue weight of the mesenteric depot is unchanged, but GHR<sup>-/-</sup> mice have a significant increase in SVF cells, total T cells, and T helper cells per gram of mesenteric tissue. Thus, while quantity of the Mes depot is unaltered, the cellular makeup of this depot is altered in GHR<sup>-/-</sup> mice. In addition, at advanced age, SubQ and Epi show subtle changes, with a decrease in cytotoxic T cells in the SubQ being the only significant difference. Because Mes was not measured at 24 months, it is unclear if the changes seen at 8 months would persist at an advanced age.

The GHR<sup>-/-</sup> mice in this study demonstrate a similar phenotype to previous reports. Specifically, GHR<sup>-/-</sup> mice weigh significantly less, have greater percentage fat mass and less percentage lean mass than WT controls (31, 32). In addition, the increase in fat mass for GHR<sup>-/-</sup> mice is not uniform, with SubQ being the only depot significantly increased relative to body weight and comparable to WT mice in absolute weight, although this difference weakens at older ages.

Depot differences in GHR<sup>-/-</sup> mice are not limited to size of the depot. In a previous report examining expression of GH-related genes in GHR<sup>-/-</sup> mice in different adipose depots (33), GHR<sup>-/-</sup> SubQ was found to have increased insulin receptor and IGF-1 receptor gene expression and decreased IGF-1 expression. GHR<sup>-/-</sup> Epi, on the other hand, have increased IGF-1 receptor gene expression, decreased IGF-1 gene expression and no change in insulin receptor expression, while GHR<sup>-/-</sup> Mes have increased insulin receptor and IGF-1 receptor gene expression and no change in IGF-1 expression. Other depot differences are well established in these mice (for review see Berryman et al (34)).

Interestingly, despite being the only enlarged depot and the depot with the most consistently changed GH-related gene expression, there was only one genotype difference in SubQ immune cell populations and only at one age. In accordance with our results, a previous study found increased expression of genes related to nonimmune cells, such as fibroblasts, endothelial and stromal cells in SubQ WAT of GHR<sup>-/-</sup> mice compared to controls (35). These data suggest that the specific immune cells analyzed here do not contribute to the unique expansion of the SubQ depot in GHR<sup>-/-</sup> mice and instead point towards the importance of the other SVF cells not identified in this study (Figure 7). Examples of these unexamined SVF cells could include fibroblasts, preadipocytes,(36) beige adipocytes,(37) endothelial cells, stem cells, and some additional immune cells, such as B cells, mast cells, dendritic cells, and eosinophils. The difference that we observed in SubQ was a significant decrease in the cytotoxic T cell population in GHR<sup>-/-</sup> mice at 24 months of age, cells which have previously been reported to be involved in initiation of adipose tissue inflammation (38). The decrease in cytotoxic T cells result could help explain the lack of changes seen in macrophage infiltration in this model. The SubQ WAT phenotype observed not only demonstrates that GH levels have different action on immune infiltration on different depots, but also suggests that GH can shape the inflammatory infiltrate in WAT. This result is particularly interesting taking into account the characteristics of healthy obesity observed in GHR<sup>-/-</sup> mice.

The epididymal depot has a decrease in total SVF cells, but no change is observed when normalized to tissue weight. This suggests that the total SVF cell population changes along with depot size. In accordance with this, in the epididymal depot, there are no significant changes in the normalized number of cells in any of the cell types that were measured at either age. This is despite a significant decrease in the weight of the depot. The disconnect between WAT mass and immune cell alterations is further supported by the results observed in the mesenteric depot. The mesenteric depot is the most consistently changed in GHR<sup>-/-</sup> mice regarding immune cells despite no change in tissue weight. GHR<sup>-/-</sup> Mes WAT has increased SVF cells normalized to tissue weight, and despite no observed difference in leukocytes or antigen presenting cells, GHR<sup>-/-</sup> Mes has increased T cells and T helper cells compared to wild type, with no changes in activated macrophages or macrophage subsets. Because we could not distinguish between T helper cell subsets in this experiment, it is unclear the functional significance of the increase in T helper cells in the context of WAT inflammation.

Monocyte-macrophage populations are plastic and can differentiate into various subsets according to changes in the environment (39). Although no differences in total ATMs were observed in SubQ, a previous study recently reported a decrease in SubQ ATMs compared to controls (17). Interestingly, the previous study used 12 month old GHR<sup>-/-</sup> mice, an intermediate age to the ones used in the current study, but an additional marker was used for ATMs, which could explain the discrepancy between the previous study and the current one. Like total activated ATMs, M1 macrophages were unchanged in all three depots of GHR<sup>-/-</sup> mice. M1 macrophages are pro-inflammatory and are usually associated with not only obesity but also metabolic dysfunction of WAT (40). The lack of increase in pro-inflammatory macrophages and the decrease in cytotoxic T cells in the WAT of GHR<sup>-/-</sup> mice despite their obesity could help explain their 'healthy' obesity phenotype. M2



macrophages were also unchanged at both ages and in all three depots. In contrast to *GHR*<sup>-/-</sup> mice, bGH transgenic mice have increased M2 macrophages in all depots, which is interesting because M2 macrophages are generally anti-inflammatory and are associated with healthy WAT, but bGH mice are less healthy than *GHR*<sup>-/-</sup> mice and have dysfunctional WAT. M2 macrophages are also implicated in tissue remodeling, however, and the excess collagen deposition in WAT of bGH mice (41) may explain the increase seen in M2 macrophages. It is important to note that there is a large spectrum of ATMs, all with distinct phenotypes (42), and the binary categorization into M1 or M2 overlooks some of the complexity of macrophage phenotypes. Overall, these results indicate that WAT health is more complex than can be described by examining macrophage populations alone.

Studies in bGH and *GHR*<sup>-/-</sup> mice have previously shown that GH alters T cell number and function in various tissues. For example, *GHR*<sup>-/-</sup> mice have an increase in naïve T cell populations in the spleen at an old age (17). Here, we show T helper cells are increased in Mes in *GHR*<sup>-/-</sup> mice. However, we did not distinguish between T helper subsets such as Th1, Th2 or Th17 cells. Further investigation into these subsets may be interesting as Th2 cells are associated with reversal of chronic inflammation, and transplantation of Th2 cells reverses weight gain and insulin resistance in obese mice (43–45). Data from our lab show that excess GH in bGH mice significantly alters pathways related to T cell activation and infiltration in the SubQ depot (16). In addition, increases in cytotoxic T cells, which are known producers of IL-6, TNF- $\alpha$  and IL-1 $\beta$  (46), have been demonstrated in WAT (Epi) of bGH mice. The *GHR*<sup>-/-</sup> mice demonstrate a decrease in the cytotoxic T cell population in the SubQ, at least at older ages. Collectively, these studies in mice with altered GH indicate that T cell populations in WAT are a major target of GH action and should be the focus of further studies that explore the immune cell subsets. The flow cytometry results of the bGH mice and both ages of *GHR*<sup>-/-</sup> mice are summarized in Figure 8.

Individuals with obesity often experience chronic, systemic, low grade inflammation in addition to WAT inflammation. This chronic inflammation is related to the pathology of obesity (47). *GHR*<sup>-/-</sup> mice are generally healthy despite their obesity, demonstrated by their increased lifespan (23). In addition to the lack of immune cell infiltration in *GHR*<sup>-/-</sup> WAT, *GHR*<sup>-/-</sup> mice lack chronic systemic inflammation, as measured by the serum cytokines IL-6, MCP-1, and TNF- $\alpha$ . In fact, the *GHR*<sup>-/-</sup> mice have a 50% decrease in TNF- $\alpha$  ( $p=0.075$ ), indicating that they may have decreased systemic inflammation at 8 months of age, although the no change is seen at the older age.

In summary, flow cytometry was used to quantify the number of immune cell populations in WAT depots in 8- and 24-month-old *GHR*<sup>-/-</sup> mice compared to WT controls. We saw a large increase in the quantity of the SubQ WAT, but subtle changes to the immune cells. Mes WAT showed opposite results, with no change in quantity but many changes in immune populations. Therefore, it is likely that other SVF cells or immune cells not identified in this experiment play a larger role in expansion of the SubQ depot. The depot differences in immune cells we observed could have potential physiological implications, such as has been reported with decreased fertility when Epi is depleted(48) or the divergent adipogenesis profiles of each depot(49). In addition, functional studies will be important to determine the

metabolic phenotype, the pathogen sensing machinery, and the immune cell trafficking mechanisms in the absence of GH in WAT immune cells.

## Supplementary Material

Refer to Web version on PubMed Central for supplementary material.

## iv. ACKNOWLEDGEMENTS

**Funding:** This work was supported in part by NIH grant #AG059779, the College of Health Sciences and Professions Student Research Grant, Ohio University Heritage College of Osteopathic Medicine, The Diabetes Institute at Ohio University, and the State of Ohio's Eminent Scholar Program that includes a gift from Milton and Lawrence Goll.

## Abbreviations:

<b>GH</b>	growth hormone
<b>GHR<sup>-/-</sup></b>	growth hormone receptor knockout
<b>WAT</b>	white adipose tissue
<b>SVF</b>	stromal vascular fraction
<b>ATMs</b>	adipose tissue macrophages
<b>SubQ</b>	subcutaneous
<b>bGH</b>	bovine growth hormone
<b>Epi</b>	epididymal
<b>Mes</b>	mesenteric
<b>NMR</b>	nuclear magnetic resonance
<b>FMO</b>	fluorescence minus one
<b>APCs</b>	antigen presenting cells
<b>WT</b>	wild type
<b>CCR2</b>	chemokine (C-C motif) receptor 2

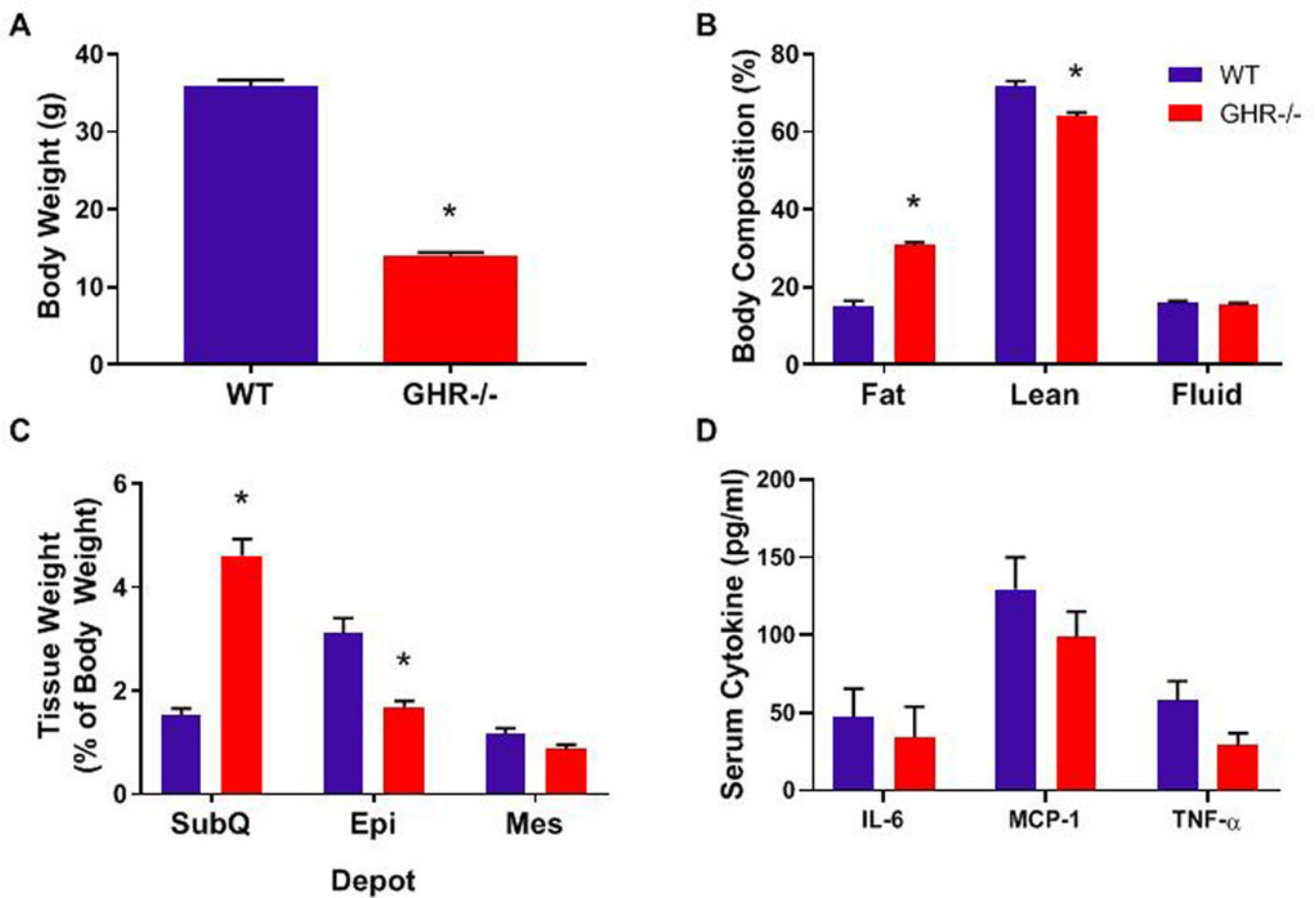
## vii. REFERENCES

1. Smith PE. The effect of hypophysectomy upon the involution of the thymus in the rat. *The Anatomical Record*. 1930; 47(1): 119–29.
2. Dhahbi J, Li X, Tran T, Masternak MM, Bartke A. Circulating blood leukocyte gene expression profiles: Effects of the Ames dwarf mutation on pathways related to immunity and inflammation. *Exp Gerontol*. 2007; 42(8): 772–88. [PubMed: 17611063]
3. Bartke A Can growth hormone (GH) accelerate aging? Evidence from GH-transgenic mice. *Neuroendocrinology*. 2003; 78210–6.
4. Smaniotto S, Alves Martins-Neto A, Dardenne M, Savino W. Growth hormone is a modulator of lymphocyte migration. *Neuroimmunomodulation*. 2011; 18(5): 309–13. [PubMed: 21952682]

5. Wang Z, Masternak MM, Al-Regaiey KA, Bartke A. Adipocytokines and the regulation of lipid metabolism in growth hormone transgenic and calorie-restricted mice. *Endocrinology*. 2007; 148(6): 2845–53. [PubMed: 17347312]
6. Deepak D, Daousi C, Javadpour M, Clark D, Perry Y, Pinkney J, MacFarlane IA. The influence of growth hormone replacement on peripheral inflammatory and cardiovascular risk markers in adults with severe growth hormone deficiency. *Growth Hormone and IGF Research*. 2010; 20(3): 220–5. [PubMed: 20185347]
7. Choe SS, Huh JY, Hwang IJ, Kim JI, Kim JB. Adipose Tissue Remodeling: Its Role in Energy Metabolism and Metabolic Disorders. *Front Endocrinol (Lausanne)*. 2016; 730.
8. Lumeng CN, Bodzin JL, Saltiel AR. Obesity induces a phenotypic switch in adipose tissue macrophage polarization. *Journal of Clinical Investigation*. 2007; 117(1): 175–84. [PubMed: 17200717]
9. Wensveen FM, Jeleni V, Valenti S, Šestan M, Wensveen TT, Theurich S, Glasner A, Mendrila D, Štimac D, Wunderlich FT, Brüning JC, Mandelboim O, Poli B. NK cells link obesity-induced adipose stress to inflammation and insulin resistance. *Nature immunology*. 2015; 16(4): 376–85. [PubMed: 25729921]
10. Wensveen FM, Valenti S, Šestan M, Turk Wensveen T, Poli B. The “Big Bang” in obese fat: Events initiating obesity-induced adipose tissue inflammation. *European Journal of Immunology*. 2015; 452446–56.
11. Mau T, Yung R. Adipose tissue inflammation in aging. *Exp Gerontol*. 2018; 10527–31.
12. Flin DJ, Binart N, Boumard S, Kopchick JJ, Kelly P. Developmental aspects of adipose tissue in GH receptor and prolactin receptor gene disrupted mice: Site-specific effects proliferation, differentiation and hormone sensitivity. *Journal of Endocrinology*. 2006; 191(1): 101–11. [PubMed: 17065393]
13. Kelder B, Berryman DE, Clark R, Li A, List EO, Kopchick JJ. CIDE-A gene expression is decreased in white adipose tissue of growth hormone receptor/binding protein gene disrupted mice and with high-fat feeding of normal mice. *Growth Hormone & IGF Research*. 2007; 17(4): 346–51. [PubMed: 17544797]
14. Lu C, Kumar PA, Sun J, Aggarwal A, Fan Y, Sperling MA, Lumeng CN, Menon RK. Targeted deletion of growth hormone (GH) receptor in macrophage reveals novel osteopontin-mediated effects of GH on glucose homeostasis and insulin sensitivity in diet-induced obesity. *J Biol Chem*. 2013; 288(22): 15725–35.
15. Masternak MM, Bartke A, Wang F, Spong A, Gesing A, Fang Y, Salmon AB, Hughes LF, Liberati T, Boparai R, Kopchick JJ, Westbrook R. Metabolic effects of intra-abdominal fat in GHRKO mice. *Aging Cell*. 2012; 11(1): 73–81. [PubMed: 22040032]
16. Benencia F, Harshman S, Duran-Ortiz S, Lubbers ER, List EO, Householder L, Al-Naeeli M, Liang X, Welch L, Kopchick JJ, Berryman DE. Male bovine GH transgenic mice have decreased adiposity with an adipose depot-specific increase in immune cell populations. *Endocrinology*. 2015; 156(5): 1794–803. [PubMed: 25521584]
17. Spadaro O, Goldberg EL, Camell CD, Youm YH, Kopchick JJ, Nguyen KY, Bartke A, Sun LY, Dixit VD. Growth Hormone Receptor Deficiency Protects against Age-Related NLRP3 Inflammasome Activation and Immune Senescence. *Cell Rep*. 2016; 14(7): 1571–80. [PubMed: 26876170]
18. Kumari M, Heeren J, Scheja L. Regulation of immunometabolism in adipose tissue. *Semin Immunopathol*. 2018; 40(2): 189–202. [PubMed: 29209828]
19. Li C, Xu MM, Wang K, Adler AJ, Vella AT, Zhou B. Macrophage polarization and meta-inflammation. *Transl Res*. 2018; 19129–44.
20. Masternak MM, Darcy J, Victoria B, Bartke A. Dwarf Mice and Aging. *Progress in Molecular Biology and Translational Science*. 2018; 15569–83.
21. Guevara-Aguirre J, Balasubramanian P, Guevara-Aguirre M, Wei M, Madia F, Cheng CW, Hwang D, Martin-Montalvo A, Saavedra J, Ingles S, De Cabo R, Cohen P, Longo VD. Growth hormone receptor deficiency is associated with a major reduction in pro-aging signaling, cancer, and diabetes in humans. *Science translational medicine*. 2011; 3(70): 70ra13–70ra13.

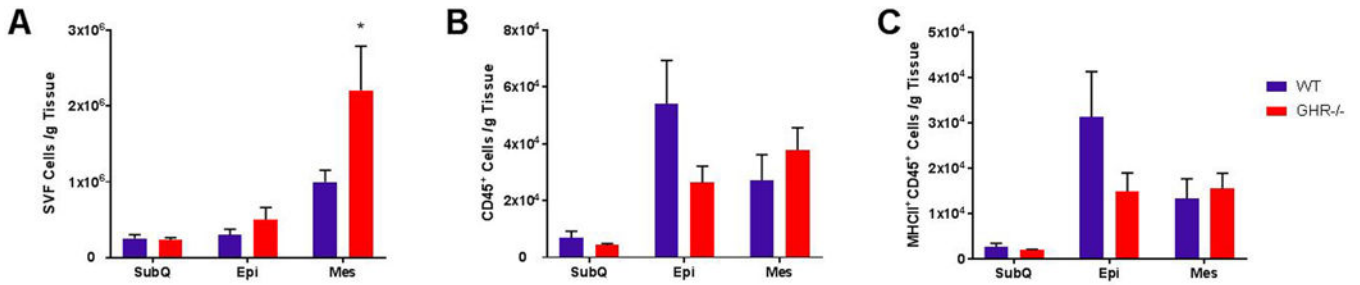
22. Ikeno Y, Hubbard GB, Lee S, Cortez LA, Lew CM, Webb CR, Berryman DE, List EO, Kopchick JJ, Bartke A. Reduced incidence and delayed occurrence of fatal neoplastic diseases in growth hormone receptor/binding protein knockout mice. *Journals of Gerontology - Series A Biological Sciences and Medical Sciences*. 2009; 64(5): 522–9.
23. Coschigano KT, Holland AN, Riders ME, List EO, Flyvbjerg A, Kopchick JJ. Deletion, but not antagonism, of the mouse growth hormone receptor results in severely decreased body weights, insulin, and insulin-like growth factor I levels and increased life span. *Endocrinology*. 2003; 144(9): 3799–810. [PubMed: 12933651]
24. Zhou Y, He L, Baumann G, Kopchick JJ. Deletion of the mouse GH-binding protein (mGHBP) mRNA polyadenylation and splicing sites does not abolish production of mGHBP. *Journal of molecular endocrinology*. 1997; 19(1): 1–13. [PubMed: 9278856]
25. Palmer AJ, Chung MY, List EO, Walker J, Okada S, Kopchick JJ, Berryman DE. Age-related changes in body composition of bovine growth hormone transgenic mice. *Endocrinology*. 2009; 150(3): 1353–60. [PubMed: 18948397]
26. List EO, Palmer AJ, Berryman DE, Bower B, Kelder B, Kopchick JJ. Growth hormone improves body composition, fasting blood glucose, glucose tolerance and liver triacylglycerol in a mouse model of diet-induced obesity and type 2 diabetes. *Diabetologia*. 2009; 52(8): 1647–55. [PubMed: 19468705]
27. List EO, Berryman DE, Wright-Piekarski J, Jara A, Funk K, Kopchick JJ. The effects of weight cycling on lifespan in male C57BL/6J mice. *International Journal of Obesity*. 2013; 37(8): 1088–94. [PubMed: 23229739]
28. Wang H, Shen L, Sun X, Liu F, Feng W, Jiang C, Chu X, Ye X, Wang Y, Zhang P, Zang M, Zhu D, Bi Y. Adipose group 1 innate lymphoid cells promote adipose tissue fibrosis and diabetes in obesity. *Nat Commun*. 2019; 10(1): 3254. [PubMed: 31332184]
29. Gerriets VA, MacIver NJ. Role of T cells in malnutrition and obesity. *Frontiers in Immunology*. 2014; 5(AUG): 379-. [PubMed: 25157251]
30. Morris DL, Singer K, Lumeng CN. Adipose tissue macrophages: phenotypic plasticity and diversity in lean and obese states. *Current opinion in clinical nutrition and metabolic care*. 2011; 14(4): 341–6. [PubMed: 21587064]
31. Berryman DE, List EO, Coschigano KT, Behar K, Kim JK, Kopchick JJ. Comparing adiposity profiles in three mouse models with altered GH signaling. *Growth Hormone & IGF Research*. 2004; 14309–18.
32. Berryman DE, List EO, Palmer AJ, Chung MY, Wright-Piekarski J, Lubbers E, O'Connor P, Okada S, Kopchick JJ. Two-year body composition analyses of long-lived GHR null mice. *Journals of Gerontology - Series A Biological Sciences and Medical Sciences*. 2010; 65(1): 31–40.
33. Hjortebjerg R, Berryman DE, Comisford R, Frank SJ, List EO, Bjerre M, Frystyk J, Kopchick JJ. Insulin, IGF-1, and GH Receptors Are Altered in an Adipose Tissue Depot-Specific Manner in Male Mice With Modified GH Action. *Endocrinology*. 2017; 158(5): 1406–18. [PubMed: 28323915]
34. Berryman DE, List EO. Growth Hormone's Effect on Adipose Tissue: Quality versus Quantity. *Int J Mol Sci*. 2017; 18(8).
35. Stout MB, Tchkonina T, Pirtskhalava T, Palmer AK, List EO, Berryman DE, Lubbers ER, Escande C, Spong A, Masternak MM, Oberg AL, LeBrasseur NK, Miller RA, Kopchick JJ, Bartke A, Kirkland JL. Growth hormone action predicts age-related white adipose tissue dysfunction and senescent cell burden in mice. *Aging (Albany NY)*. 2014; 6(7): 575–86. [PubMed: 25063774]
36. Lessard J, Laforest S, Pelletier M, Leboeuf M, Blackburn L, Tchernof A. Low abdominal subcutaneous preadipocyte adipogenesis is associated with visceral obesity, visceral adipocyte hypertrophy, and a dysmetabolic state. *Adipocyte*. 2014; 3(3): 197–205. [PubMed: 25068086]
37. Cohen P, Levy JD, Zhang Y, Frontini A, Kolodin DP, Svensson KJ, Lo JC, Zeng X, Ye L, Khandekar MJ, Wu J, Gunawardana SC, Banks AS, Camporez JPG, Jurczak MJ, Kajimura S, Piston DW, Mathis D, Cinti S, Shulman GI, Seale P, Spiegelman BM. Ablation of PRDM16 and beige adipose causes metabolic dysfunction and a subcutaneous to visceral fat switch. *Cell*. 2014; 156(1–2): 304–16. [PubMed: 24439384]

38. Nishimura S, Manabe I, Nagasaki M, Eto K, Yamashita H, Ohsugi M, Otsu M, Hara K, Ueki K, Sugiura S, Yoshimura K, Kadowaki T, Nagai R. CD8+ effector T cells contribute to macrophage recruitment and adipose tissue inflammation in obesity. *Nature medicine*. 2009; 15(8): 914–20.
39. Yang J, Zhang L, Yu C, Yang XF, Wang H. Monocyte and macrophage differentiation: Circulation inflammatory monocyte as biomarker for inflammatory diseases. *Biomarker Research*. 2014; 21-. [PubMed: 25789166]
40. Lumeng CN, Delproposto JB, Westcott DJ, Saltiel AR. Phenotypic switching of adipose tissue macrophages with obesity is generated by spatiotemporal differences in macrophage subtypes. *Diabetes*. 2008; 57(12): 3239–46. [PubMed: 18829989]
41. Householder LA, Comisford R, Duran-Ortiz S, Lee K, Troike K, Wilson C, Jara A, Harberson M, List EO, Kopchick JJ, Berryman DE. Increased fibrosis: A novel means by which GH influences white adipose tissue function. *Growth Horm IGF Res*. 2018; 3945–53.
42. Patel AN, Yockman J, Vargas V, Bull DA. Putative population of adipose-derived stem cells isolated from mediastinal tissue during cardiac surgery. *Cell transplantation*. 2013; 22(3): 507–11. [PubMed: 22490339]
43. Constant SL, Bottomly K. Induction of Th1 and Th2 CD4 + T cell responses: The alternative approaches. *Annual Review of Immunology*. 1997; 15(1): 297–322.
44. Molofsky AB, Nussbaum JC, Liang H-E, Van Dyken SJ, Cheng LE, Mohapatra A, Chawla A, Locksley RM. Innate lymphoid type 2 cells sustain visceral adipose tissue eosinophils and alternatively activated macrophages. *The Journal of experimental medicine*. 2013; 210(3): 535–49. [PubMed: 23420878]
45. Stolarczyk E, Lord GM, Howard JK. The immune cell transcription factor T-bet: A novel metabolic regulator. *Adipocyte*. 2014; 3(1): 58–62. [PubMed: 24575371]
46. Esser N, Legrand-Poels S, Piette J, Scheen AJ, Paquot N. Inflammation as a link between obesity, metabolic syndrome and type 2 diabetes. *Diabetes Research and Clinical Practice*. 2014; 105141–50.
47. Ellulu MS, Patimah I, Khaza'ai H, Rahmat A, Abed Y. Obesity and inflammation: the linking mechanism and the complications. *Arch Med Sci*. 2017; 13(4): 851–63. [PubMed: 28721154]
48. Chu Y, Huddleston GG, Clancy AN, Harris RB, Bartness TJ. Epididymal fat is necessary for spermatogenesis, but not testosterone production or copulatory behavior. *Endocrinology*. 2010; 151(12): 5669–79. [PubMed: 20881242]
49. Caesar R, Manieri M, Kelder T, Boekschoten M, Evelo C, Muller M, Kooistra T, Cinti S, Kleemann R, Drevon CA. A combined transcriptomics and lipidomics analysis of subcutaneous, epididymal and mesenteric adipose tissue reveals marked functional differences. *PLoS One*. 2010; 5(7): e11525.



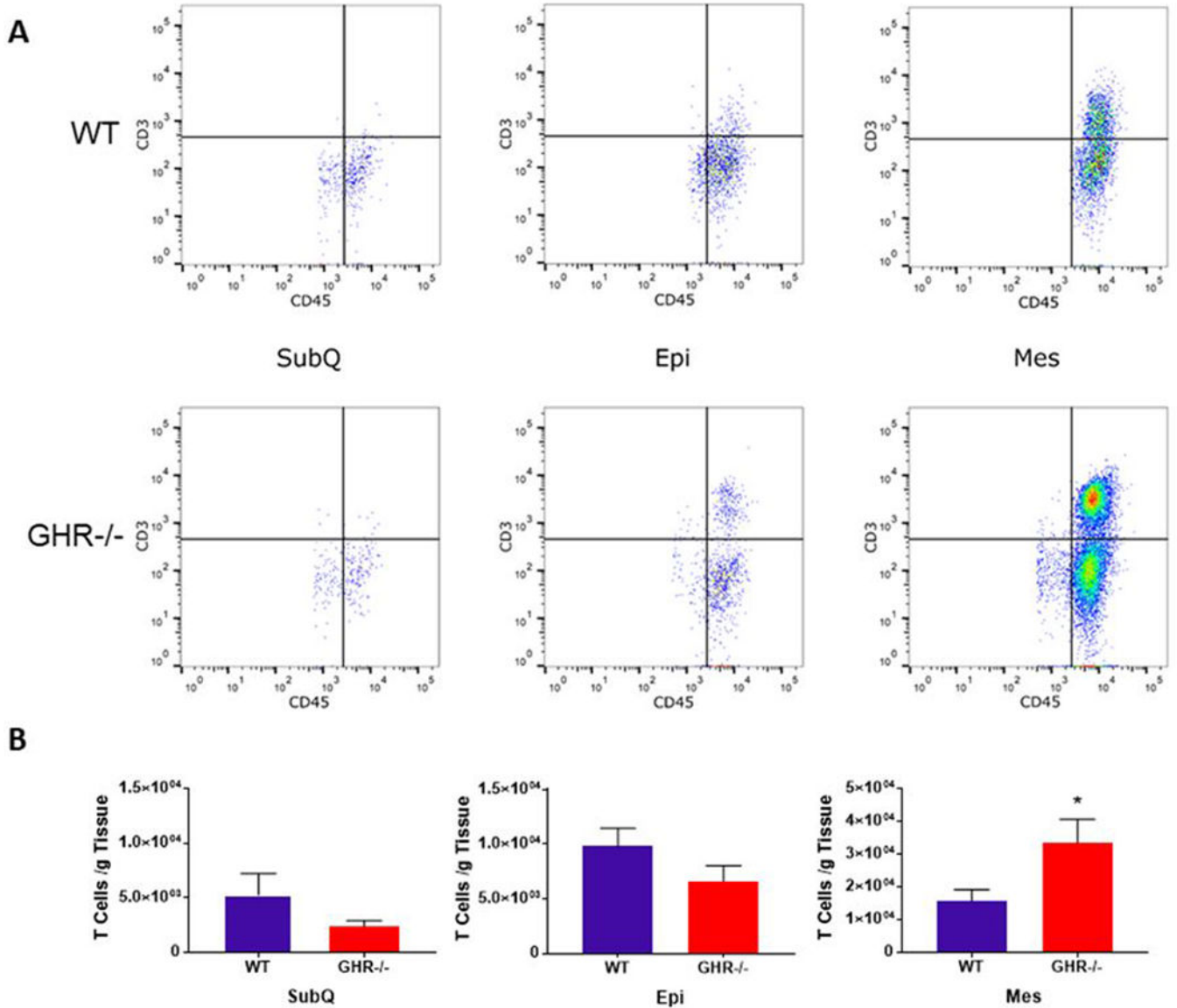
**Figure 1.**

Characteristics of 8-month-old WT and GHR<sup>-/-</sup> mice. A. Body weight,  $p < 0.0001$ ,  $t = 22.17$ ,  $df = 13$ . B. Body composition as percent of body weight: Fat  $p < 0.0001$ ,  $t = 10.47$ ,  $df = 13$ ; Lean  $p = 0.0004$ ,  $t = 4.773$ ,  $df = 13$ ; Fluid  $p = 0.1218$ ,  $t = 1.655$ ,  $df = 13$ . C. Adipose tissue depot weights expressed as percent of total body weight: SubQ  $p < 0.0001$ ,  $t = 9.126$ ,  $df = 13$ ; Epi  $p = 0.0018$ , Welch-corrected  $t = 4.326$ ,  $df = 9.289$ ; Mes  $p = 0.0446$ ,  $t = 2.223$ ,  $df = 13$ . D. Serum cytokine levels: IL-6  $p = 0.3969$ ,  $U = 20$ ; MCP-1  $p = 0.2654$ ,  $t = 1.937$ ,  $df = 13$ ; TNF $\alpha$   $p = 0.075$ ,  $t = 1.937$ ,  $df = 13$ . Data are expressed as mean  $\pm$  SEM. WT  $n = 8$  and GHR<sup>-/-</sup>  $n = 8$ . \* indicates a significant difference;  $p < 0.05$ .



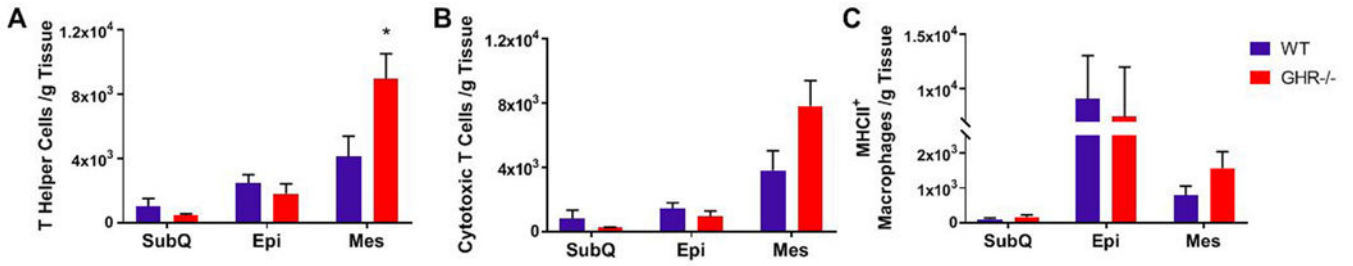
**Figure 2.**

Quantification of SVF, CD45+ leukocytes, and MHC-II antigen presenting cells in 8 month old WT and GHR<sup>-/-</sup> mice. A. Estimated total SVF cells normalized to gram of WAT: SubQ  $p=0.6903$ ,  $t=0.4075$ ,  $df=13$ ; Epi  $p=0.2552$ ,  $t=1.2$ ,  $df=11$ ; Mes  $p=0.014$ ,  $U=7$ . B. Number of CD45+ cells per gram of tissue: SubQ  $p=0.6943$ ,  $U=24$ ; Epi  $p=0.1226$ , Welch-corrected  $t=1.705$ ,  $df=8.955$ ; Mes  $p=0.2345$ ,  $U=20$ . C. Number of activated (MHC-II+) CD45+ cells normalized to gram of WAT: SubQ  $p=0.4634$ ,  $U=21$ ; Epi  $p=0.065$ ,  $U=14$ ; Mes  $p=0.6454$ ,  $U=27$ . Data are expressed as mean  $\pm$  SEM. WT  $n = 8$  and GHR<sup>-/-</sup>  $n = 8$ . \* indicates a significant difference;  $p < 0.05$ .



**Figure 3.** Quantification of adipose tissue T cells in WT and GHR<sup>-/-</sup> WAT depots at 8 months of age. A. Dot plot distribution of T cells (CD3<sup>+</sup> CD45<sup>+</sup>) in WT and GHR<sup>-/-</sup> male mice. The y-axis and x-axis of the dot plots represent fluorescent intensity. B. Number of CD3<sup>+</sup>CD45<sup>+</sup> T cells normalized to depot weight in WT and GHR<sup>-/-</sup> male mice: SubQ p=0.4634, U=21; Epi p=0.1304, U=17; Mes p=0.0281, U=11. Data are expressed as mean ± SEM. WT n = 8 and GHR<sup>-/-</sup> n = 8. \* indicates a significant difference; p < 0.05





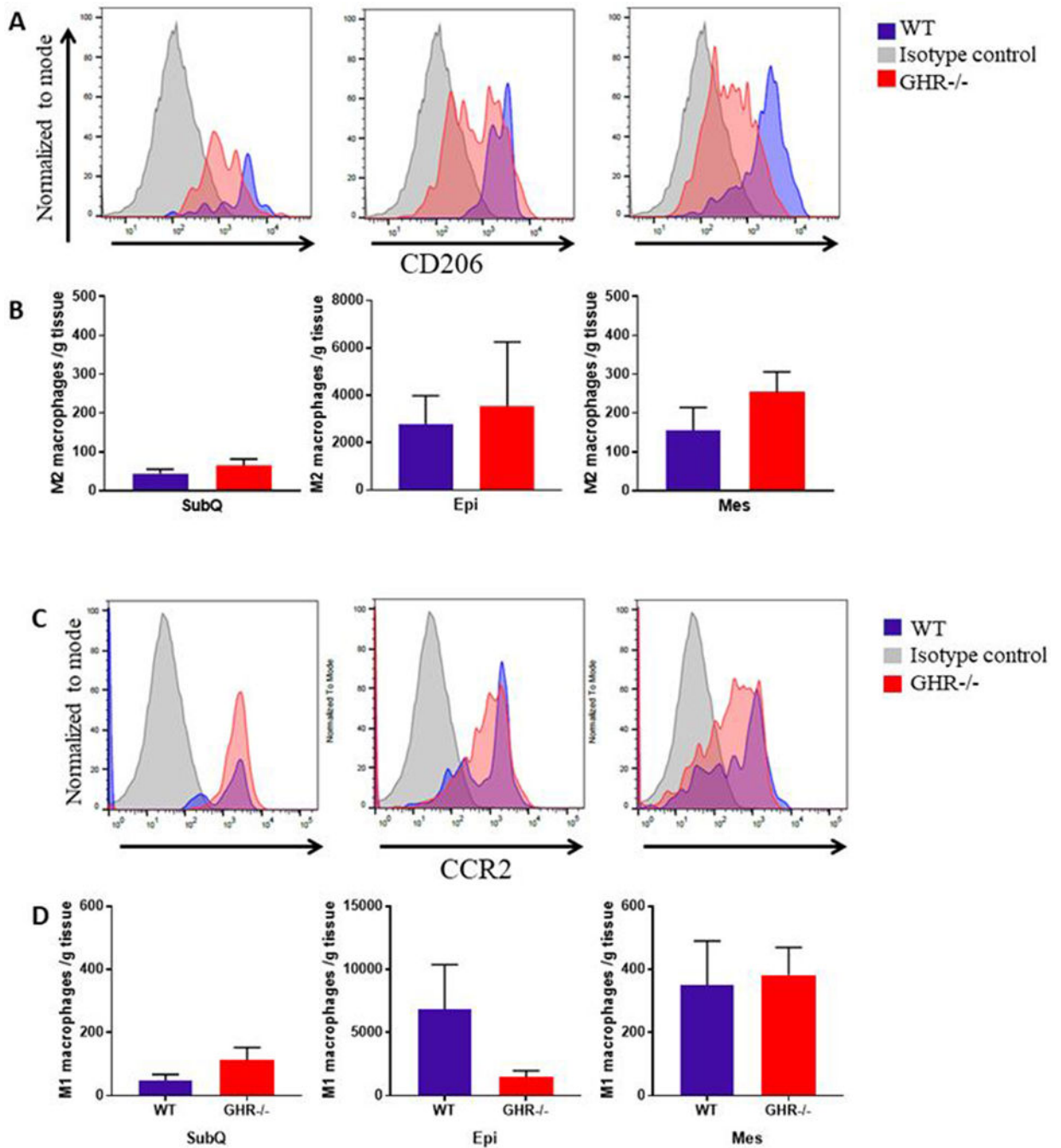
**Figure 4.** Quantification of WAT T cell subsets and MHC-II<sup>+</sup> activated adipose tissue macrophages (ATMs) at 8 months of age. A. Number of CD3<sup>+</sup>CD4<sup>+</sup> T helper cells: SubQ p=0.9551, U=27; Epi p=0.4347, t=0.8042, df=14; Mes 118% increase; p=0.0148, U=9. B. Number of CD3<sup>+</sup>CD4<sup>-</sup> cytotoxic T cells: SubQ p=0.9551, U=27; Epi p=0.2786, U=21; Mes p=0.0662, t=1.993, df=14. C. Number of MHCII<sup>+</sup> activated ATMs: SubQ p=0.4634, U=21; Epi p=0.4418, U=24; Mes p=0.1679, t=1.454, df=14. Data are reported as the mean of the number of cells per gram of tissue ± SEM. WT n = 8 and GHR<sup>-/-</sup> n = 8. \* indicates a significant difference; p < 0.05.

Author Manuscript

Author Manuscript

Author Manuscript

Author Manuscript



**Figure 5.**

Comparisons of M2 and M1 populations in WT and GHR<sup>-/-</sup> mice at 8 months of age. A and C. Distribution and quantification of M2 macrophages (A) and M1 macrophages (C) in WT and GHR<sup>-/-</sup> male mice. The y-axis represents relative number of events normalized to mode and the x-axis represents the intensity of the fluorescent signal. Isotype control, WT and GHR<sup>-/-</sup> are represented by gray, blue and red peaks respectively. B and D. Distribution and quantification of M2 macrophages (B: SubQ  $p=0.28$ ,  $t=1.127$ ,  $df=13$ ; Epi  $p=0.3823$ ,  $U=23$ ; Mes  $p=0.1605$ ,  $U=18$ ) and M1 macrophages (D: SubQ  $p=0.2319$ ,  $U=17$ ; Epi

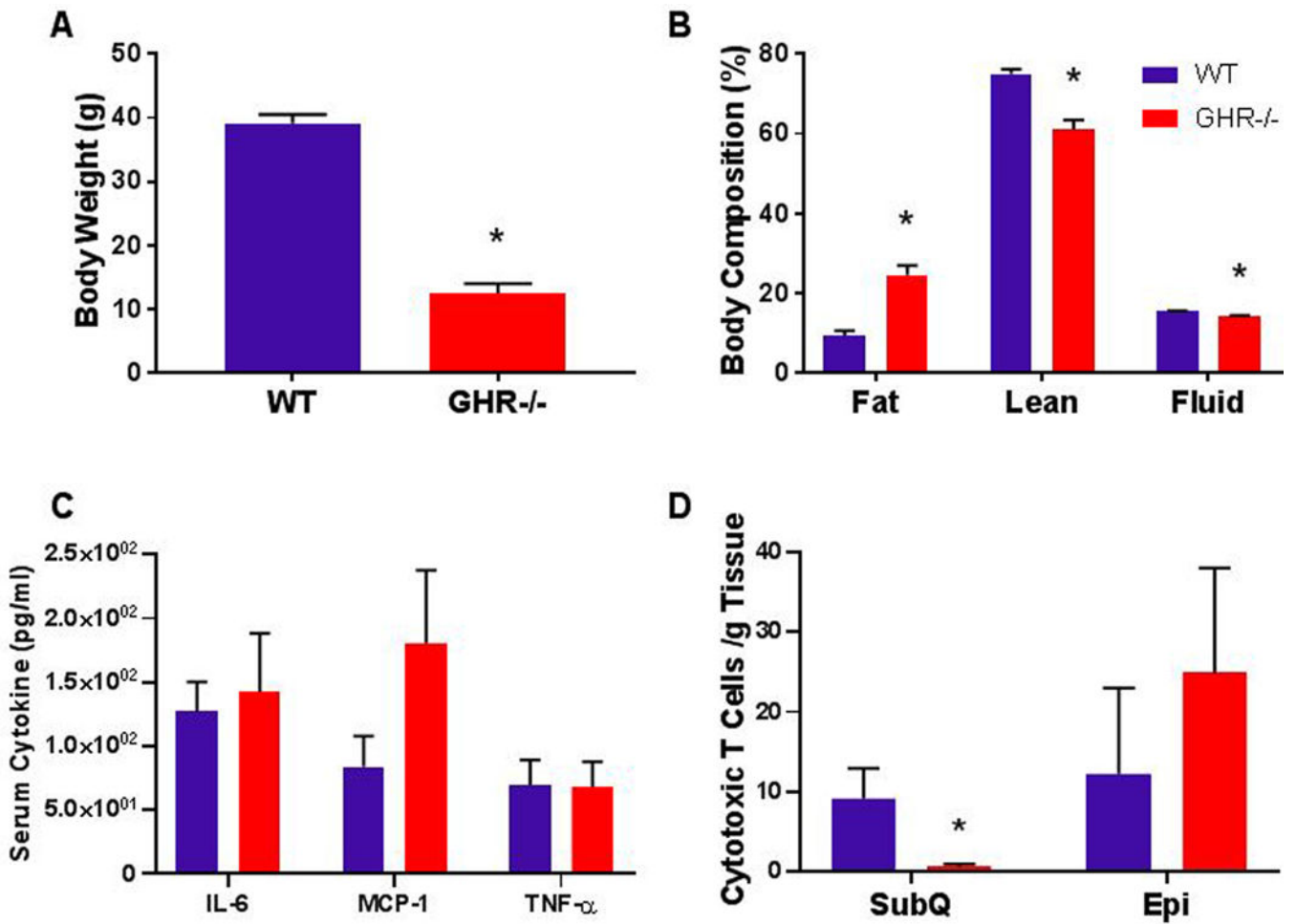
p=0.1944, U=19; Mes p=0.3823, U=23) in WT and GHR<sup>-/-</sup> male mice. M2 and M1 populations were derived from F480<sup>+</sup>CD11b<sup>+</sup>CD45<sup>+</sup> ATM parent population. It should be noted that because cells over a certain fluorescence threshold were counted, the variation in intensity of the fluorescence shown in A and C is not reflected in the enumeration of cells reported in B and D. Data are reported as the mean of the number of cells per gram of tissue  $\pm$  SEM.

Author Manuscript

Author Manuscript

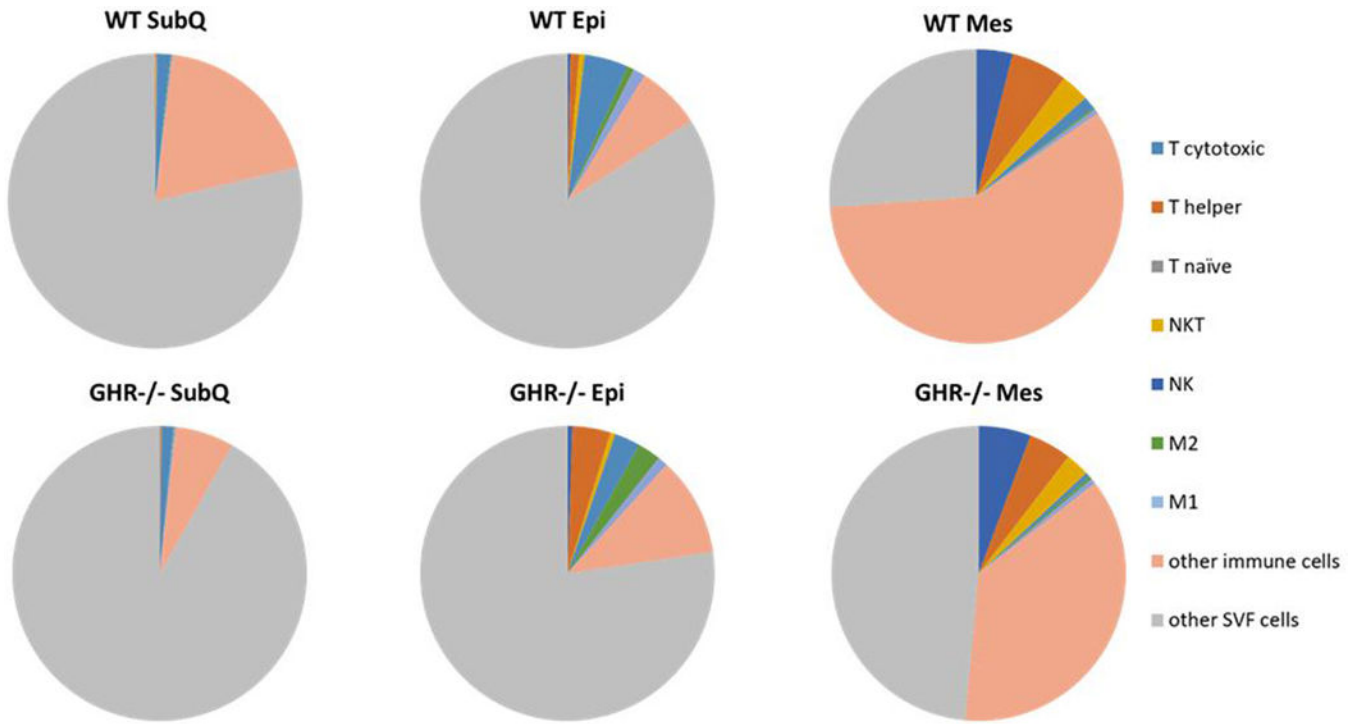
Author Manuscript

Author Manuscript



**Figure 6.**



Notable results from the 24 month cohort of GHR<sup>-/-</sup> mice. A. Body weight  $p < 0.0001$ ,  $t = 12.95$ ,  $df = 12$ . B. Body composition expressed as percent of body weight: Fat  $p < 0.0001$ ,  $t = 5.815$ ,  $df = 12$ ; lean  $p = 0.0006$ ,  $U = 0$ ; fluid  $p = 0.0024$ ,  $t = 3.826$ ,  $df = 12$ . C. Serum cytokine levels: IL-6  $p = 0.6402$ ,  $U = 27$ ; MCP-1  $p = 0.2092$ , Welch-corrected  $t = 1.356$ ,  $df = 8.704$ ; TNF- $\alpha$   $p = 0.4462$ ,  $U = 24.5$ . D. Number of CD3<sup>+</sup>CD8<sup>+</sup> cytotoxic T cells, reported as the mean of the number of cells per gram of tissue  $\pm$  SEM: SubQ  $p = 0.0105$ ,  $U = 5.5$ ; Epi  $p = 0.7523$ ,  $U = 18.5$ . WT  $n = 8$  and GHR<sup>-/-</sup>  $n = 8$ . \* indicates a significant difference;  $p < 0.05$ .


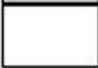


**Figure 7.** Proportion of immune cells and other SVF cells in WAT depots in WT and GHR<sup>-/-</sup> male mice at 8 months of age. Number of T cytotoxic cells, T helper cells, M1 macrophages, M2 macrophages, and other CD45<sup>+</sup> leukocytes in WT and GHR<sup>-/-</sup> male mice normalized to gram of adipose tissue. WT n = 8 and GHR<sup>-/-</sup> n = 8.

	bGH			GHR <sup>-/-</sup> 8 mo			GHR <sup>-/-</sup> 24 mo		
	SubQ	Epi	Mes	SubQ	Epi	Mes	SubQ	Epi	Mes
SVF	Increased	No Change	Increased	No Change	No Change	Increased	No Change	No Change	No Change
Leukocytes	No Change	Decreased	Increased	No Change	No Change	No Change	No Change	No Change	No Change
APCs	No Change	No Change	No Change	No Change	No Change	No Change	No Change	No Change	No Change
T cells	No Change	No Change	No Change	No Change	No Change	Increased	No Change	No Change	No Change
T helper cells	Increased	No Change	No Change	No Change	No Change	Increased	No Change	No Change	No Change
Cytotoxic T cells	No Change	Increased	Decreased	No Change	No Change	No Change	Decreased	No Change	No Change
Macrophages	Increased	No Change	Increased	No Change	No Change	No Change	No Change	No Change	No Change
M1 Macrophages	No Change	No Change	No Change	No Change	No Change	No Change	No Change	No Change	No Change
M2 Macrophages	Increased	Increased	Increased	No Change	No Change	No Change	No Change	No Change	No Change

 Increased  
 Decreased

 No Change  
 Not Measured

**Figure 8.** Summary of flow cytometry results. The flow cytometry results of three different cohorts of GH-altered mice (bGH(16), GHR<sup>-/-</sup> 8 months, and GHR<sup>-/-</sup> 24 months) are summarized in this figure. A significant increase is indicated by a blue cell, significant decrease an orange cell, no significant change is indicated by a grey cell and no measurement is a signified by a white cell.

**Table 1.**

## Flow Cytometry Antibodies (8 Months)

Target	Conjugate	Manufacturer	Catalog #	RRID
CD206	AF488	BioRad	MCA2235A488	AB_324891
Ly-6C	PerCP-Cy5.5	Thermo Fisher	45-5932-80	AB_1518762
MHC-II	Biotin	Thermo Fisher	13-5321-81	AB_466661
F4/80	PE-Cy7	Thermo Fisher	25-4801-82	AB_469653
CD11c	APC	Thermo Fisher	117-0114-81	AB_469345
CD45	APC-eFluor 780	Thermo Fisher	47-0451-82	AB_1548781
CD11b	Alexa Fluor 700	Thermo Fisher	56-0112-80	AB_657586
CCR2	Phycoerythrin	R&D Systems	FAB5538P	AB_10718414
NK1.1	FITC	Thermo Fisher	11-5941-81	AB_465317
NKT	Phycoerythrin	BD Biosciences	550082	AB_393552
CD44	Biotin	Thermo Fisher	13-0441-81	AB_466441
CD4	PerCP-Cy5.5	Thermo Fisher	45-0042-80	AB_906231
CD3	PE-Cy7	Thermo Fisher	25-0031-81	AB_469571
CD25	APC	Thermo Fisher	17-0251-81	AB_469365
CD62L	Alexa Fluor 700	Thermo Fisher	56-0621-80	AB_494004
CD45	Alexa Fluor 700	Thermo Fisher	56-0451-80	AB_891456
CD16/CD32		Thermo Fisher	14-0161-82	AB_467133
Streptavidin	eFluor 615	Thermo Fisher	42-4317-80	AB_11218079

**Table 2.**

## Flow Cytometry Antibodies (24 Months)

Target	Conjugate	Manufacturer	Catalog #	RRID
CD11b	VioGreen	Miltenyi Biotec	130-113-811	AB_2726328
CD11c	APC-Vio770	Miltenyi Biotec	130-110-841	AB_2654715
CD206	APC	BioLegend	141707	AB_10896057
CD25	PE	Miltenyi Biotec	130-108-996	AB_2656655
CD3	APC-Vio770	Miltenyi Biotec	130-109-840	AB_2657087
CD38	PE-Vio770	Miltenyi Biotec	130-109-258	AB_2657842
CD4	VioGreen	Miltenyi Biotec	130-109-413	AB_2657964
CD44	PE-Vio770	Miltenyi Biotec	130-110-085	AB_2658157
CD45	VioBlue	Miltenyi Biotec	130-110-802	AB_2658222
CD62L	PerCP-Vio700	Miltenyi Biotec	130-107-046	AB_2660523
CD80	PE	Miltenyi Biotec	130-116-460	AB_2727557
CD8a	FITC	Miltenyi Biotec	130-102-490	AB_2659883
F4/80	PerCP-Vio700	Miltenyi Biotec	130-102-161	AB_2651711
GITR	APC	Miltenyi Biotec	130-116-427	AB_2727531

Author Manuscript

Author Manuscript

Author Manuscript

Author Manuscript